

Gapless to gapless phase transitions by mode fractionalization in quantum spin chains

Shi Feng,¹ Gonzalo Alvarez,² and Nandini Trivedi¹

¹*Department of Physics, The Ohio State University, Columbus, Ohio 43210, USA*

²*Computational Sciences and Engineering Division and Center for Nanophase Materials Sciences, Oak Ridge National Laboratory, Oak Ridge, Tennessee 37831, USA*

(Dated: June 22, 2022)

We investigate spin chains with bilinear-biquadratic spin interactions as a function of an applied magnetic field h . At the Uimin-Lai-Sutherland (ULS) critical point we find a remarkable hierarchy of fractionalized excitations revealed by the dynamical structure factor $S(q, \omega)$ as a function of magnetic field yielding a transition from a gapless phase to another gapless phase before reaching the fully polarized state. At $h = 0$, the envelope of the lowest energy excitations goes soft at *two points* $q_1 = 2\pi/3$ and $q_2 = 4\pi/3$, dubbed the A-phase. With increasing field, the spectral peaks at each of the gapless points bifurcate and combine to form a new set of fractionalized excitations that soften at a *single point* $q = \pi$ at $h_{c1} \approx 0.94$. Beyond h_{c1} the system remains in this phase dubbed the B-phase until the transition at $h_{c2} = 4$ to the fully polarized phase. We discuss the central charge of these two gapless phases and contrast the behavior with that of the gapped Haldane phase in a field.

Introduction: Quantum Spin liquids (QSL) are exotic quantum phases beyond Landau's symmetry-breaking paradigm that are expected to emerge in the presence of frustration or in low dimensions whereby long-range magnetic order is suppressed by strong quantum fluctuations¹. While similar to a paramagnet, in that QSLs do not possess any long range order, they are however, a non-trivial state of matter characterized by long range entanglement that leads to a new kind of topological order². Topological order is reflected in fractionalized particles with non-trivial braiding statistics and long range topological entanglement.³⁻⁵

While non-trivial topological order is not possible in 1d systems, QSL phases arise due to the Lieb-Shultz-Mattis (LSM) theorem⁶, as the analog of Mermin-Wagner theorem, that leads to disordered states with fractionalized excitations. Moreover, the availability of rich theoretical tools in 1D systems, such as conformal field theory (CFT)^{7,8}, Luttinger liquid^{9,10} and density matrix renormalization group (DMRG)^{11,12}, makes (quasi) one dimensional spin chains an important theoretical platform to explore possible spin liquid phases and phase transitions.

One dimensional interacting systems has a long history that dates back to 1931 when the exact solution of the spin-1/2 Heisenberg chain was found by Bethe¹³, predicting quasi-long-range order in the ground state and gapless excitations. The mechanism of such gaplessness was given by the LSM theorem whereby the separation between the ground and first excited state energies of a half-integer spin chain was shown to vanish in the thermodynamic limit⁶. Haldane's generalization to larger spin S SU(2) chains, using a mapping to a non-linear sigma model, showed that one dimensional Heisenberg antiferromagnets with integer spins have an excitation gap¹⁴⁻¹⁶, later observed in experiments^{17,18}.

In this paper we discover a new phenomenon: a phase transition from a gapless QSL to another gapless QSL in a spin-1 quantum chain in an applied magnetic field. While both QSL phases harbor fractionalized excitations, their nature is different, with modes that go soft at different

points in the Brillouin zone. Given material candidates, we expect our predictions for the dynamical structure factor to be observable by inelastic neutron spectroscopy.

The Model: The general model for a system of $S = 1$ interacting spins is the bilinear-biquadratic Hamiltonian (BLBQ) defined on a chain of L sites given by:

$$H_{BLBQ} = \sum_{\langle ij \rangle} \mathbf{S}_i \cdot \mathbf{S}_j - \beta (\mathbf{S}_i \cdot \mathbf{S}_j)^2. \quad (1)$$

This model has the well-known phase diagram²¹ shown in Fig.1(a), parameterized by β or the related angle $\tan \theta = -\beta$, where $\beta = 0$ corresponds to the aforesaid spin-1 antiferromagnets. The gapped phase relevant for Haldane's conjecture, termed Haldane phase, emerges for a wide range of β as a symmetry protected topological (SPT) phase²², which disappears at the ULS point due to the closing of the gap.

Recent progress on quantum materials, has made it possible to investigate many (quasi) one-dimensional quantum magnets of spin-1 such as CsNiCl₃^{17,23,24}, LiVGe₂O₆^{25,26}, and $5d^4$ materials like OsCl₄ whose magnetic phase transition under an applied field is expected to be captured by Eq. (1) under a field at $\beta = -1$ (ULS)²⁷⁻²⁹.

Given the availability of candidate spin chain materials, adds to the importance of understanding phase transitions in such materials in an externally applied magnetic field. It was shown by Affleck that the gap of the spin-1 Heisenberg antiferromagnet at $\beta = 0$ closes at a critical magnetic field and can be understood as a Bose-Einstein condensation of magnons³⁰. In this paper our focus is to study phase transitions in the BLBQ family under an external magnetic field:

$$H = H_{BLBQ} + h \sum_i S_i^z. \quad (2)$$

We expect the magnetic-field-induced phase transitions in Eq.(2) to be first order transitions because the magnetic field term is conserved. However, that does not imply a

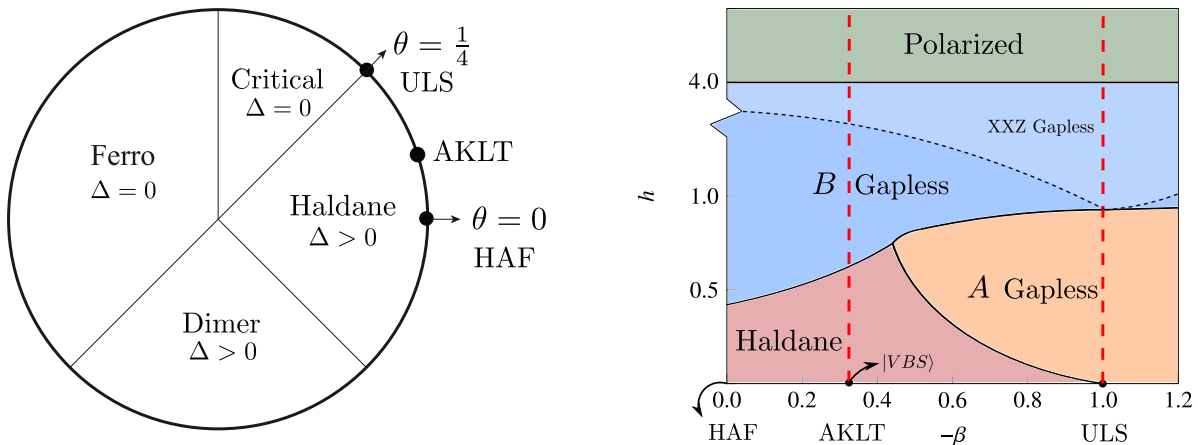


FIG. 1: Left panel: phase diagram of the spin-1 bilinear-biquadratic (BLBQ) model parameterized by the angle θ : $H = \sum_{\langle ij \rangle} \cos \theta \mathbf{S}_i \cdot \mathbf{S}_j + \sin \theta (\mathbf{S}_i \cdot \mathbf{S}_j)^2$. Δ denotes the gap which can be zero or finite in different phases. We focus on two representative points: the Affleck-Kennedy-Lieb-Tasaki (AKLT) model at $\theta \approx 0.1024\pi$ ($\beta = -1/3$), and the critical ULS model at $\theta = \pi/4$ ($\beta = -1$). VBS refers to the valence bond solid ground state of the AKLT model at $h = 0$. The Heisenberg antiferromagnetic model at $\theta = 0$ ($\beta = 0$) is discussed in the Supplement¹⁹. Right panel: schematic phase diagram of BLBQ parameterized by β and h reproduced from Ref.²⁰. Phase boundaries are marked by black solid lines. black dashed line marks a cross-over to an effective spin-1/2 XXZ model in a field within the B phase; at $-\beta = 1$ the mapping is to an effective spin-1/2 Heisenberg model. We obtain the evolution of the static and dynamical correlation functions in the gapless A-phase, B-phase and Haldane phase along the two red dashed lines (AKLT and ULS).

simple transition to a polarized phase by a level crossing at large field. In fact, intermediate phases, termed S1 and S2 that reflect the number of modes by Fath and Littlewood, have been found to intervene over a large range of fields between the state at zero field and the fully polarized phase^{20,31}, with a crossover to an effective spin-1/2 XXZ model within S1-phase^{32,33}. Yet as we show below, the term S2 phase must be modified since the 2 modes of the ULS state bifurcate once put under a non-zero field; hence we dub these instead phase A and B phase in this paper. The schematic phase diagram is shown in Fig.1(b).

Because the field term is conserved, the ground state of the model at a particular value of β with a field then becomes the ground state of a block Hamiltonian with a fixed S_z of the model without a field. We perform numerical calculations using DMRG for lattice sizes up to 200 sites with periodic and open boundary conditions.

Main Results: While these intermediate phases were identified more than a decade ago, in this paper we identify the mechanisms underlying these phase transitions. We focus on the Uimin-Lai-Sutherland (ULS) critical point $\beta = -1$ ³⁴⁻³⁶ marked in the figure Fig.1(b), which shows a remarkable *phase transition from a gapless phase to another gapless phase*. We first see this from the power law nature of the static correlations. In our central result in Fig. 2 we show the behavior of the dynamical structure factor in a field that reveals the *mechanism* of the gapless to gapless phase transition.

We discover a hierarchy of fractionalized excitations that evolve from two broad peaks that soften at $q_1 = 2\pi/3$

and $q_2 = 4\pi/3$ at zero field in the first gapless phase dubbed A, start bifurcating at finite field, and beyond a critical field $h_{c1} \approx 1$ combine to form new fractionalized excitations that now soften at a $q = \pi$ in the second gapless phase, dubbed the B phase. The fractionalized nature of the excitations and their evolution from one gapless phase to the other are the core of our results. We discuss below the reasons behind the robustness of the A phase even in the absence of a gap, and the mapping of the spin-1 model to the effective spin-1/2 Heisenberg model in a field in the B phase which provides understanding of the dynamical spectral functions.

Entanglement Entropy: The von Neumann entanglement entropy S_{vN} of a subsystem A with the rest of the chain is obtained from the reduced density matrix ρ_A of the ground state $|g.s.\rangle$ ^{37,38}:

$$\begin{aligned} \rho_A &= \text{Tr}_B [|g.s.\rangle \langle g.s. |], \\ S_{vN} &= -\text{Tr} [\rho_A \log(\rho_A)] \end{aligned} \quad (3)$$

Fig.2(a,b) shows a first order transition of the average magnetization in a field that is directly reflected in the discontinuity of the entanglement entropy, which shows a jump from $S_{vN} \approx 2$ in the A-phase to $S_{vN} \approx 1$ in the B-phase at $h_{c1} \approx 0.94$. The transition to the fully polarized phase occurs at $h_{c2} = 4$ where S_{vN} goes to zero.

The spin-spin correlations show power law behavior in both A and B phases Figure 2(c,d), consistent with both being gapless phases. The static structure factor $S(q)$ has a 2-peak structure in the A-phase (4-peak with field) and

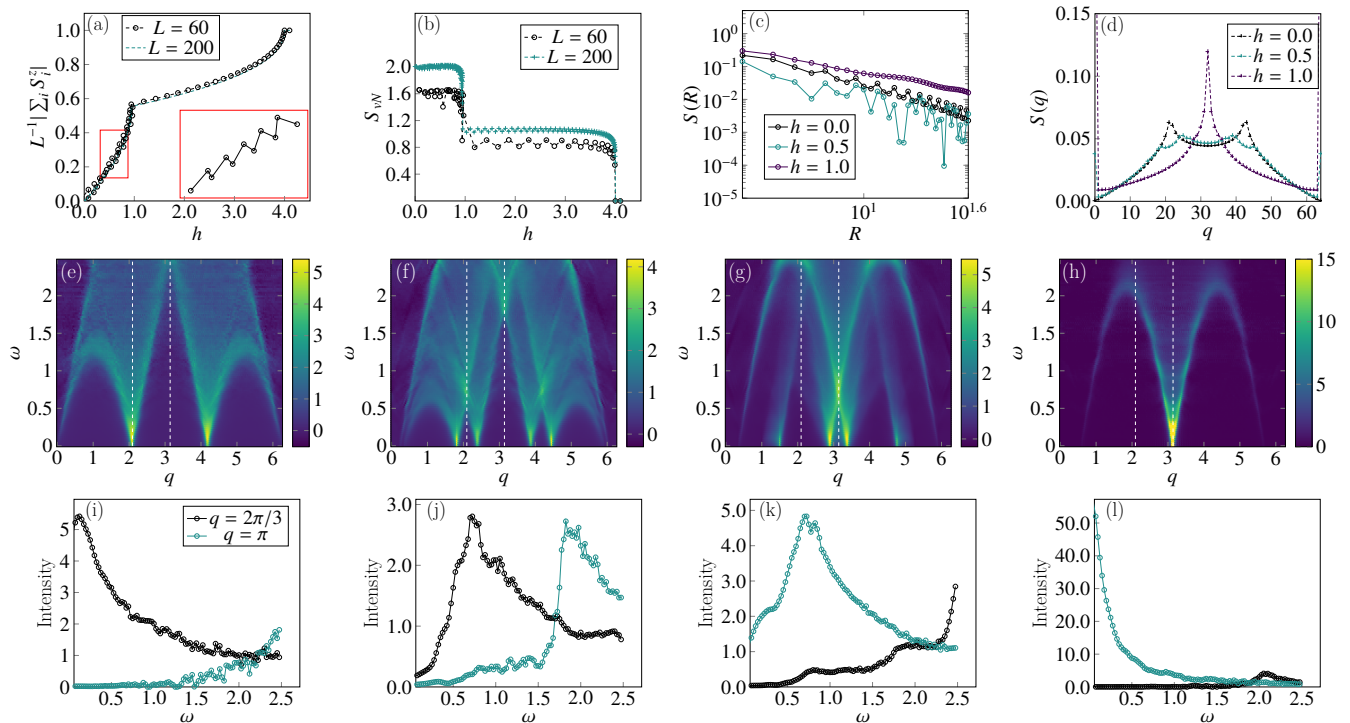


FIG. 2: BLBQ model at the critical ULS point as a function of a magnetic field h . The critical field of ULS model is $h_{c1} \approx 0.94$ (a) Magnetization per site m with an inset showing a zoom-in of m in the A-phase indicated by the red square. (b) von-Neumann entanglement entropy S_{vN} for a cut at the central bond. (c) Real space spin-spin correlation function at $h = 0, 0.5$ in the A-phase, and $h = 1.0$ in the B-phase showing power law decay in both phases. (d) The Fourier transform $S(q)$ of the correlation functions showing the 2 to 4-peak structure in the A-phase and the 1-peak structure in the B phases. Results in (a), (b) are obtained with DMRG on a 60-site lattice and 200-site lattice (as indicated) under OBC; (c), (d) are obtained using 64-site DMRG under OBC for the ULS model. (e-h) $S^{+-}(q, \omega)$ dynamics of ULS model at field $h = 0$ ($s_z = 1/200$), $h = 0.5$ ($s_z \approx 0.16$), $h = 0.9$ ($s_z \approx 0.50$), and $h = 1.5$ ($s_z \approx 0.60$). (i-l) cuts of $S^{+-}(k, \omega)$ at the soft mode $q = 2\pi/3$ and the antiferromagnetic mode $q = \pi$ shown by white dashed lines in the previous row.

a single peak in the B phase. The main question we want to understand in this paper is how can these two phases be distinguished? And moreover, what is the mechanism of this gapless to gapless transition?

Dynamical Correlations The dynamical correlation function is obtained from the spatial and time Fourier transform of the time-dependent spin-spin correlation function $S^{\alpha,\beta}(q, \omega) = FT \langle S_j^\alpha(t) S_j^\beta(0) \rangle$. Figure 2(e-h) shows the $S^+ S^-$ component of the dynamical structure factor calculated using DMRG for a lattice of 200 sites with open boundary conditions, with and without field h , as indicated. (The $S^z S^z$ and $S^- S^+$ components are shown in the Supplement¹⁹) Before the first transition at h_{c1} , the dynamical structure factor $S(q, \omega)$ in Fig.2(e) shows that a wide range of frequencies are excited at a given momentum, in contrast to the gapped Haldane phase that has sharper modes that can be captured by single mode approximation^{19,39–42}. At low energies, the spectrum for the ULS model has two gapless incommensurate modes at $q \sim 2\pi/3, 4\pi/3$ corresponding to the two peaks in the static structure factor shown in Fig. 2(d) at $h = 0$. The broad spectrum provides clear evidence for fractionalized

excitations.

Adding a field breaks the $SU(3)$ symmetry of the ULS model into $U(1) \times U(1)$. As shown in Fig. 2(f), this reduction of symmetry is accompanied by the bifurcation of the two incommensurate “modes” that are both 2-fold degenerate, resulting in 4 distinct gapless “modes”. Given the large range of frequencies over which the spectral weight at a given q is spread over, these are clearly not well-defined modes. However, there is considerable concentration of spectral weight that soften at the incommensurate momenta $2\pi/3$ and $4\pi/3$. Upon increasing the field, we find that the two pairs of modes move in opposite directions in momentum space. Near h_{c1} one pair of modes recombines into a degenerate mode at π , the other pair moves further away from each other and becomes fainter as the field reaches h_{c1} . Finally, as shown in Fig. 2(h), at $h = 1.5 > h_{c1}$ we see only the gapless mode at π while the other pair is completely washed out. As discussed below, the evolution of the dynamical structure factor shows explicitly how the bifurcation and recombination of degenerate soft modes yields a spectrum that shows strong similarities with that of the spin-1/2 Heisenberg model.

Robustness of A-phase: In the absence of a gap protecting the A phase, what is the reason behind the robustness of the A-phase up to a critical field h_{c1} ? As we show next, we can exploit the SU(3) symmetry of the ULS Hamiltonian to show explicitly the stability of the gapless A-phase and the transition at h_{c1} . For this purpose, it is useful to map the ULS Hamiltonian onto a fermion model, in which spin-1 operators are decomposed into partons by the mapping $\mathbf{S}_i \equiv \psi_i^\dagger \mathbf{S}_i \psi_i$ with $\psi_i = (b_{i,1}, b_{i,0}, b_{i,-1})$ describing 3 annihilation components of a fermionic spinor corresponding to $m = 1, 0, -1$. We follow the fermionizing approach of Ref.⁴³ to show that the ULS Hamiltonian (with some auxiliary constants) can be written as

$$H_{ULS} - c = \sum_{\langle ij \rangle} \mathbf{S}_i \cdot \mathbf{S}_j + (\mathbf{S}_i \cdot \mathbf{S}_j)^2 - c$$

$$= - \sum_{\langle ij \rangle; mm'} b_{i,m}^\dagger b_{j,m} b_{j,m'}^\dagger b_{i,m'}$$
(4)

where we have defined the auxiliary diagonal term $c = n_i n_j + 3n_i$ with $n_i = \sum_m b_{im}^\dagger b_{im}$ being the total *on-site* occupation number operator. (A more complete derivation can be found in the Supplement¹⁹). The fermionic representation reveals the larger symmetry than is apparent, without having to write H_{ULS} in terms of generators of the Lie algebra of SU(3). Equation (4) can be compactly written as $-\sum_{\langle ij \rangle} (\psi_i^\dagger \psi_j) (\psi_j^\dagger \psi_i)$. This expression is invariant under any symmetry transformations in $\{U \in GL(3, \mathbb{C}) | U^\dagger U = \mathbb{I}, \det(U) = 1\} = SU(3)$, which directly shows the SU(3) symmetry of the ULS point. From this representation, we see three conserved quantities, by computing the following commutators

$$[\hat{N}_m, H_{ULS}] \equiv \left[\sum_i b_{i,m}^\dagger b_{i,m}, H_{ULS} \right] = 0, \quad (5)$$

where we have defined \hat{N}_m to be the total occupation number operator of m -type fermion of the whole lattice. Let N_m be the eigenvalue of \hat{N}_m , which must be an integer because it is a good quantum number. We can hereafter identify N_{-1} as the number of sites with $m = -1$, N_0 the number of sites with $m = 0$, and N_1 number of sites with $m = 1$. The ULS model then conserves N_0 , N_1 , and N_{-1} *separately*. Because the sum of the three equals the number of sites L , there are *two* linearly independent quantities (l.i.); thus the ULS model has *two* local symmetries.

Let us choose the total Sz and the total N_1 : $[H_{ULS}, Sz] = [H_{ULS}, N_1] = 0$. A field h in the z direction does not change these symmetries, because $\sum_i S_i^z = \sum_i b_{i,1}^\dagger b_{i,1} - b_{i,-1}^\dagger b_{i,-1}$ obviously commutes with all N_m . We can then label the energy of the ULS in each block (Sz, N_1) with $E_{ULS}(Sz, N_1)$, and the energy of the ULS *with* field as $E_{ULS}(Sz, N_1) + hSz$.

Because we choose $h \geq 0$, N_1 tends to decrease as h increases, and Sz tends to become more negative, so that $|Sz|$ increases as h increases. For $h < h_{c1}$, the system

can decrease its energy by either increasing $|Sz|$, or, by decreasing N_1 , or, both. Decreasing N_1 while at the same time increasing $|Sz|$ increases $E_{ULS}(Sz, N_1)$ but decreases hSz , so the two terms compete.

At first, it costs more to constantly increase $|Sz|$, and the system must instead zigzag $|Sz|$ as is shown in the inset figure of Fig.2(a). But at some large enough field h , the field term wins and decreasing $|Sz|$ is no longer advantageous energetically. This happens when N_1 cannot be decreased any further, that is, when N_1 reaches its minimum value: zero. This point marks the first order phase transition at $h = h_{c1}$. From $h > h_{c1}$ onward, there are no longer ground states with $m = 1$ sites, the magnetization Sz equals $-N_{-1}$, and $N_1 = 0$.

Cross-over to effective spin 1/2 model: It is worth pointing out that the dynamical structure factor of this $S = 1$ chain at $h = 1.5$ in Fig. 2(h) shows a fan emanating from the gapless point $q = \pi$ to higher energies with decreasing spectral weight, which resembles that of a $S = 1/2$ chain^{13,44-46}. Such behavior can be understood from a bond operator representation of spin-1^{32,33} whereby the spin states anti-parallel to the applied field can be projected out, and the spin operators can be approximated by

$$\frac{S^+}{\sqrt{2}} \sim u^\dagger t_z \equiv S^+, \quad \frac{S^-}{\sqrt{2}} \sim t_z^\dagger u \equiv S^-,$$

$$S^z \sim \frac{1}{2}(u^\dagger u - t_z^\dagger t_z) + \frac{1}{2} \equiv S^z + \frac{1}{2}$$
(6)

where t_z^\dagger creates a triplet state of spin-1/2 bond by $t_z^\dagger |0\rangle = 1/\sqrt{2}(|\uparrow\downarrow\rangle + |\downarrow\uparrow\rangle)$ and u^\dagger the bosonic creation operator defined by $u^\dagger |0\rangle = |\uparrow\uparrow\rangle$. Eq. (6) is the Schwinger boson representation of the pseudo-spin-1/2 operators. Applying such projection produces an effective spin-1/2 anisotropic Heisenberg model subjected to an effective magnetic field:

$$H_{eff} \propto \sum_{\langle ij \rangle} S_i^x S_j^x + S_i^y S_j^y + \Delta S_i^z S_j^z + h_{eff} \sum_i S_i^z \quad (7)$$

where $h_{eff} = (h - \beta - 1)/2$ and $\Delta = (1 - \beta)/2$. This explains the resemblance between the spin-1/2 system and spin-1 system after the cross-over shown in Fig.1(b). Such a mapping from the spin-1 system to the spin-1/2 system is exact³³ for $\beta = -1$ at $h > h_{c1}$, so, at fields small but larger than h_{c1} we should expect the dynamical structure factor of the B phase of ULS to coincide with that of the spin-1/2 model calculated by Bethe ansatz. For larger fields before saturation, the model is equivalent to a spin-1/2 model under an effective field $h_{eff}(h, \beta)$ whose dynamical intensity weight remains large at $\omega(q = \pi) \rightarrow 0$ but diminishes at high energy.

Comparison with the SPT phase: It is useful to compare the evolution of the dynamical correlations at the ULS critical point with that of the gapped Haldane phase. We investigate the AKLT point as a representative of the

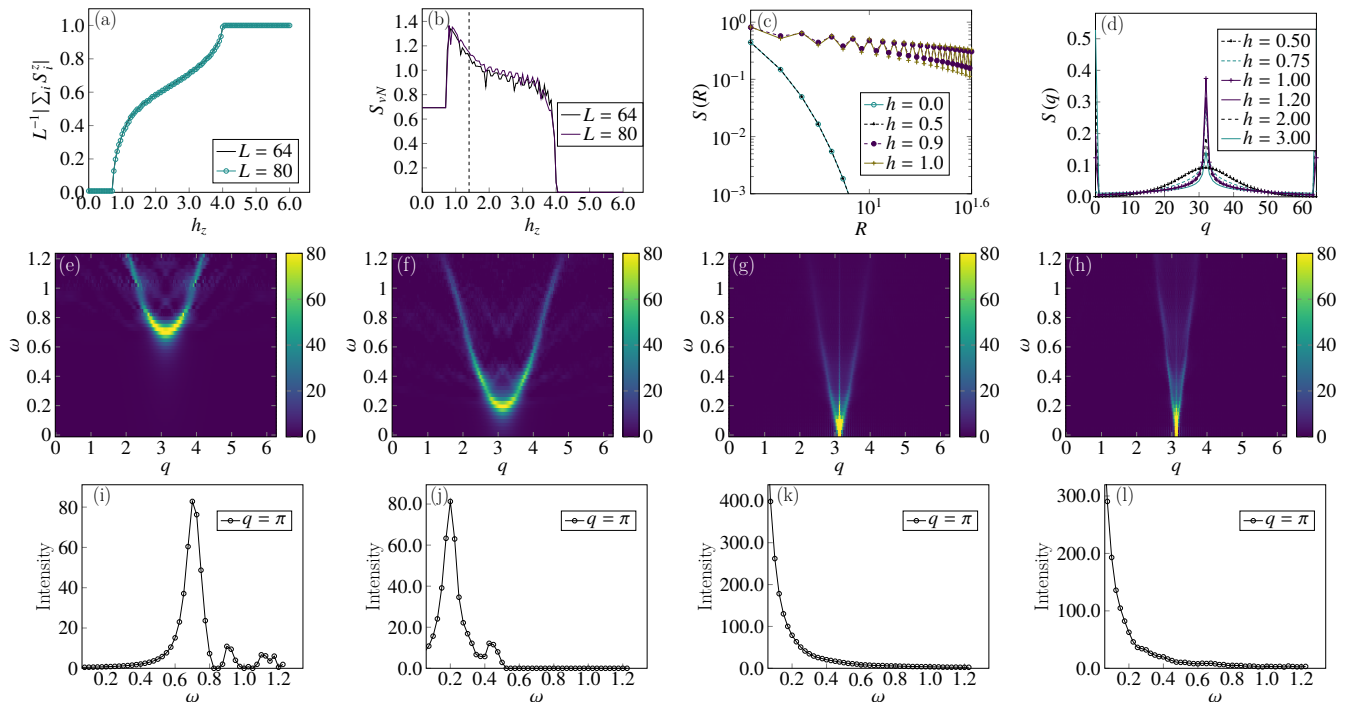


FIG. 3: BLBQ model for gapped AKLT model as a function of field h . The critical field of AKLT model is $h_{c1} \approx 0.75$ (a) Magnetization per site s_z as a function of $h \geq 0$, showing two first-order phase transitions. (b) von Neumann entanglement entropy S_{vN} for the same set of system sizes. The vertical dashed is an estimate of the cross-over field (c) Real space correlation functions at $h = 0.0, 0.5$ for the gapped SPT phase showing exponential decay, and $h = 0.9, 1.0$ for the gapless B phase with power law correlations. (d) Static structure factor in A and B phases. Data of (a-d) are obtained using 64-site DMRG under OBC. (e - h): $S^{+-}(q, \omega)$ at field $h = 0$ ($s_z = 1/200$), $h = 0.5$ ($s_z = 1/200$), $h = 1.0$ ($s_z \approx 0.3$), and at field $h = 1.5$ ($s_z \approx 0.5$). (i-l) cuts of $S^{+-}(k, \omega)$ at anti-ferromagnetic mode $q = \pi$ in $S^{+-}(q, \omega)$ shown in the previous row. Dynamical structure factors are obtained by 200-site DMRG under OBC.

Haldane phase. Its Hamiltonian reads:

$$H_{aklt} = \sum_{\langle ij \rangle} \mathbf{S}_i \cdot \mathbf{S}_j + \frac{1}{3} (\mathbf{S}_i \cdot \mathbf{S}_j)^2 \quad (8)$$

The ground state of AKLT Hamiltonian is given by the well-known valance bond solid (VBS) state⁴⁷ and is classified as a symmetry protected topological (SPT) phase protected by time-reversal, parity, and translation symmetries²². While some of the eigenstates of the AKLT model can be constructed explicitly⁴⁸⁻⁵⁰, it is helpful to obtain the complete dynamical signatures contained in the spectral function in order to compare with that of the ULS model discussed above.

When put under the external field, the dynamics of the AKLT model for $h < h_{c1}$ is similar to that at $h = 0$ because the gap at $k = \pi$ for $h = 0$ in the SPT phase protects the ground state. The gap decreases *linearly with* h , and touches zero at $h = h_{c1}$ with a spectrum akin to the B phase of the ULS model. This phase transition from a gapped to gapless phase is understandable, in contrast to the gapless to gapless transition of the ULS discussed previously. There are also differences between the two models as seen from their entanglement properties.

Figure 3(b) shows von Neumann entanglement entropy as a function of h at central bond. At small fields the gapped

SPT ground state is unchanged, and $S_{vN} = \log 2$ due to the pair of dangling spin-1/2 bonds at both ends. There is a jump upwards in S_{vN} at the SPT-S1 transition at h_{c1} followed by a gradual reduction with increasing field within the B phase followed by a transition at $h_{c2} = 4$ to zero in the high field product state. It is important to note that the decreasing S_{vN} in the B phase of the AKLT model is qualitatively different from that of the ULS model in which S_{vN} is constant in the entire phase (see Fig.2(b)).

Discussion and Outlook: In the gapless phases, the central charge provides insight into the effective underlying conformal field theory (CFT). The entanglement entropy of 1+1 dimensional CFT under OBC satisfies the Calabrese-Cardy formula:

$$S(n) = S^{CFT}(n) + S^{OSC}(n) + \text{const} \quad (9)$$

where n is the bond position. The first two terms $S^{CFT}(n)$ and $S^{OSC}(n)$ are defined as^{7,8}

$$S^{CFT}(n) = \frac{c}{6} \log \left[\frac{2L}{\pi} \sin \left(\frac{\pi n}{L} \right) \right] \quad (10)$$

$$S^{OSC}(n) = \sum_a F^a \left(\frac{n}{L} \right) \frac{\cos(2a\pi n/L)}{|L \sin(n\pi/L)|^{\Delta_a}}$$

where $c = N - 1$ and Δ_a is the central charge and the scaling dimension of the SU(N) WZW theory, N defines the SU(N) symmetry of the effective CFT, L the total length of chain, and, $F^a(n/L)$ a universal scaling factor which can be treated approximately as a constant during the fitting procedure to extract c with only one scaling dimension $a = 1$ for SU(2) and SU(3)^{51,52}.

It is well-known that in the continuum limit an antiferromagnetic spin-1/2 chain can be described by an SU(2) Wess-Zumino-Witten (WZW) theory with central charge $c = 1$, which can be generalized to many other 1+1-dimensional quantum critical systems with higher SU(N) symmetries with central charge $c = N - 1$. Based on this we expect that in the A-phase at $h = 0$ with SU(3) symmetry the central charge should be 2. The B-phase of the ULS model with $\beta = -1$ for $h_{c1} < h < h_{c2}$ can be mapped *exactly* to a spin-1/2 Heisenberg model^{32,33}, hence this intermediate phase should have an effective WZW theory with central charge $c = 1$.

While central charge of the ULS model in the entire intermediate B phase is expected to be exactly $c = 1$ due to its mapping to the spin-1/2 Heisenberg chain, such an exact mapping is no longer valid for β away from $\beta = -1$. Nonetheless, we find that the central charge as obtained by the Calabrese-Cardy formula remains $c \approx 1$ for the most part in the B phase.

Our predictions open doors for inelastic neutron scattering experiments on candidate materials pertaining to BLBQ models, taking the explorations beyond the Heisenberg $S = 1$ magnets. Future theoretical work will involve the nature of edge modes of BLBQ models under open

boundary conditions. It is also interesting to expand the search to quantum magnetic models in higher dimensions. For the Kitaev model on the honeycomb lattice, we have recently found that that in a magnetic field there is a gapless phase with a spinon Fermi surface sandwiched between a gapped non-abelian Kitaev QSL and a fully polarized phase^{53,54}. Developing an understanding of novel topologically ordered phases in 2D via coupled chain constructions could provide useful insights.

I. ACKNOWLEDGEMENT

We thank Subhro Bhattacharjee for insightful discussions. We also thank E. Miles Stoudenmire for help with the Intelligent Tensor Library (ITensor) open source code. Most of the results for the static results were obtained with ITensor⁵⁵; the dynamics (real frequency) results were obtained with DMRG++⁵⁶; see also¹⁹. S.F. and N.T. acknowledge support from DOE grant DE-FG02-07ER46423. Computations were performed using the Unity cluster at the Ohio State University and at the Ohio supercomputing center (OSC). G.A. was supported by the Scientific Discovery through Advanced Computing (SciDAC) program funded by U.S. Department of Energy, Office of Science, Advanced Scientific Computing Research and Basic Energy Sciences, Division of Materials Sciences and Engineering. GA was also supported by the ExaTN ORNL LDRD.

-
- ¹ P. W. ANDERSON, Science **235**, 1196 (1987), ISSN 0036-8075, <https://science.sciencemag.org/content/235/4793/1196.full.pdf>, URL <https://science.sciencemag.org/content/235/4793/1196>.
- ² X.-G. Wen, Phys. Rev. B **65**, 165113 (2002), URL <https://link.aps.org/doi/10.1103/PhysRevB.65.165113>.
- ³ D. C. Tsui, H. L. Stormer, and A. C. Gossard, Phys. Rev. Lett. **48**, 1559 (1982), URL <https://link.aps.org/doi/10.1103/PhysRevLett.48.1559>.
- ⁴ X. G. Wen and Q. Niu, Phys. Rev. B **41**, 9377 (1990), URL <https://link.aps.org/doi/10.1103/PhysRevB.41.9377>.
- ⁵ A. Kitaev, Annals of Physics **321**, 2 (2006), ISSN 0003-4916, January Special Issue, URL <http://www.sciencedirect.com/science/article/pii/S0003491605002381>.
- ⁶ E. Lieb, T. Schultz, and D. Mattis, Annals of Physics **16**, 407 (1961), ISSN 0003-4916, URL <http://www.sciencedirect.com/science/article/pii/0003491661901154>.
- ⁷ P. Calabrese and J. Cardy, Journal of Statistical Mechanics: Theory and Experiment **2004**, P06002 (2004), URL <https://doi.org/10.1088%2F1742-5468%2F2004%2F06%2Fp06002>.
- ⁸ P. Calabrese, M. Campostrini, F. Essler, and B. Nienhuis, Phys. Rev. Lett. **104**, 095701 (2010), URL <https://link.aps.org/doi/10.1103/PhysRevLett.104.095701>.
- ⁹ T. Giamarchi, *Quantum Physics in One Dimension*, The international series of monographs on physics 121 (Oxford University Press, 2003), ISBN 9780198525004.
- ¹⁰ M. Klanjšek, H. Mayaffre, C. Berthier, M. Horvatić, B. Chiari, O. Piovesana, P. Bouillot, C. Kollath, E. Orignac, R. Citro, et al., Phys. Rev. Lett. **101**, 137207 (2008), URL <https://link.aps.org/doi/10.1103/PhysRevLett.101.137207>.
- ¹¹ S. R. White, Phys. Rev. Lett. **69**, 2863 (1992), URL <https://link.aps.org/doi/10.1103/PhysRevLett.69.2863>.
- ¹² S. R. White, Phys. Rev. B **48**, 10345 (1993), URL <https://link.aps.org/doi/10.1103/PhysRevB.48.10345>.
- ¹³ H. Bethe, Zeitschrift für Physik **71**, 205 (1931), ISSN 0044-3328, URL <https://doi.org/10.1007/BF01341708>.
- ¹⁴ F. Haldane, Physics Letters A **93**, 464 (1983), ISSN 0375-9601, URL <http://www.sciencedirect.com/science/article/pii/037596018390631X>.
- ¹⁵ F. D. M. Haldane, Phys. Rev. Lett. **50**, 1153 (1983), URL <https://link.aps.org/doi/10.1103/PhysRevLett.50.1153>.
- ¹⁶ I. Affleck, Journal of Physics: Condensed Matter **1**, 3047 (1989), URL <https://doi.org/10.1088%2F0953-8984%2F1%2F19%2F001>.

- ¹⁷ W. J. L. Buyers, R. M. Morra, R. L. Armstrong, M. J. Hogan, P. Gerlach, and K. Hirakawa, Phys. Rev. Lett. **56**, 371 (1986), URL <https://link.aps.org/doi/10.1103/PhysRevLett.56.371>.
- ¹⁸ R. M. Morra, W. J. L. Buyers, R. L. Armstrong, and K. Hirakawa, Phys. Rev. B **38**, 543 (1988), URL <https://link.aps.org/doi/10.1103/PhysRevB.38.543>.
- ¹⁹ See Supplemental Material at [URL will be inserted by publisher] for a description and usage of the computer code.
- ²⁰ G. Fáth and P. B. Littlewood, Phys. Rev. B **58**, R14709 (1998), URL <https://link.aps.org/doi/10.1103/PhysRevB.58.R14709>.
- ²¹ A. Läuchli, G. Schmid, and S. Trebst, Phys. Rev. B **74**, 144426 (2006), URL <https://link.aps.org/doi/10.1103/PhysRevB.74.144426>.
- ²² Z.-C. Gu and X.-G. Wen, Phys. Rev. B **80**, 155131 (2009), URL <https://link.aps.org/doi/10.1103/PhysRevB.80.155131>.
- ²³ Z. Tun, Buyers, W. J. L., Armstrong, R. L., Hirakawa, K., and B. Briat, Phys. Rev. B **42**, 4677 (1990), URL <https://link.aps.org/doi/10.1103/PhysRevB.42.4677>.
- ²⁴ I. A. Zaliznyak, S.-H. Lee, and S. V. Petrov, Phys. Rev. Lett. **87**, 017202 (2001), URL <https://link.aps.org/doi/10.1103/PhysRevLett.87.017202>.
- ²⁵ P. Millet, F. Mila, F. C. Zhang, M. Mambrini, A. B. Van Oosten, V. A. Pashchenko, A. Sulpice, and A. Stepanov, Phys. Rev. Lett. **83**, 4176 (1999), URL <https://link.aps.org/doi/10.1103/PhysRevLett.83.4176>.
- ²⁶ J. Lou, T. Xiang, and Z. Su, Phys. Rev. Lett. **85**, 2380 (2000), URL <https://link.aps.org/doi/10.1103/PhysRevLett.85.2380>.
- ²⁷ O. N. Meetei, W. S. Cole, M. Randeria, and N. Trivedi, Phys. Rev. B **91**, 054412 (2015), URL <https://link.aps.org/doi/10.1103/PhysRevB.91.054412>.
- ²⁸ S. Feng, N. D. Patel, P. Kim, J. H. Han, and N. Trivedi, Phys. Rev. B **101**, 155112 (2020), URL <https://link.aps.org/doi/10.1103/PhysRevB.101.155112>.
- ²⁹ M. A. McGuire, Q. Zheng, J. Yan, and B. C. Sales, Phys. Rev. B **99**, 214402 (2019), URL <https://link.aps.org/doi/10.1103/PhysRevB.99.214402>.
- ³⁰ I. Affleck, Phys. Rev. B **43**, 3215 (1991), URL <https://link.aps.org/doi/10.1103/PhysRevB.43.3215>.
- ³¹ H. Kiwata, Journal of Physics: Condensed Matter **7**, 7991 (1995), URL <https://doi.org/10.1088%2F0953-8984%2F7%2F41%2F008>.
- ³² H.-T. Wang, J.-L. Shen, and Z.-B. Su, Phys. Rev. B **56**, 14435 (1997), URL <https://link.aps.org/doi/10.1103/PhysRevB.56.14435>.
- ³³ H.-T. Wang, H. Q. Lin, and J.-L. Shen, Phys. Rev. B **61**, 4019 (2000), URL <https://link.aps.org/doi/10.1103/PhysRevB.61.4019>.
- ³⁴ B. Sutherland, Phys. Rev. B **12**, 3795 (1975), URL <https://doi.org/10.1103/PhysRevB.12.3795>.
- ³⁵ G. V. Uimin, JETP Letters **12**, 225 (1970), URL http://www.jetpletters.ac.ru/ps/1730/article_26296.shtml.
- ³⁶ C. K. Lai, J. Math. Phys. **15**, 1675 (1974), URL <https://doi.org/10.1063/1.1666522>.
- ³⁷ M. A. Nielsen and I. L. Chuang, *Quantum Computation and Quantum Information: 10th Anniversary Edition* (Cambridge University Press, 2010).
- ³⁸ H. Li and F. D. M. Haldane, Phys. Rev. Lett. **101**, 010504 (2008), URL <https://link.aps.org/doi/10.1103/PhysRevLett.101.010504>.
- ³⁹ D. P. Arovas, A. Auerbach, and F. D. M. Haldane, Phys. Rev. Lett. **60**, 531 (1988), URL <https://link.aps.org/doi/10.1103/PhysRevLett.60.531>.
- ⁴⁰ E. S. Sørensen and I. Affleck, Phys. Rev. B **49**, 15771 (1994), URL <https://link.aps.org/doi/10.1103/PhysRevB.49.15771>.
- ⁴¹ A. D. J. (auth.), T. L. Ainsworth, C. E. Campbell, B. E. Clements, and E. K. (eds.), *Recent Progress in Many-Body Theories: Volume 3* (Springer US, 1992), 1st ed., ISBN 978-1-4613-6535-8, 978-1-4615-3466-2.
- ⁴² O. Golinelli, T. Jolicœur, and E. S. Sørensen, The European Physical Journal B - Condensed Matter and Complex Systems **11**, 199 (1999), ISSN 1434-6036, URL <https://doi.org/10.1007/BF03219165>.
- ⁴³ Y. Q. Li, M. Ma, D. N. Shi, and F. C. Zhang, Phys. Rev. Lett. **81**, 3527 (1998), URL <https://link.aps.org/doi/10.1103/PhysRevLett.81.3527>.
- ⁴⁴ M. Mourigal, M. Enderle, A. Klöpperpieper, J.-S. Caux, A. Stunault, and H. M. Rønnow, Nature Physics **9**, 435 (2013), ISSN 1745-2481, URL <https://doi.org/10.1038/nphys2652>.
- ⁴⁵ B. Lake, D. A. Tennant, J.-S. Caux, T. Barthel, U. Schollwöck, S. E. Nagler, and C. D. Frost, Phys. Rev. Lett. **111**, 137205 (2013), URL <https://link.aps.org/doi/10.1103/PhysRevLett.111.137205>.
- ⁴⁶ B. Lake, D. A. Tennant, C. D. Frost, and S. E. Nagler, Nature Materials **4**, 329 (2005), ISSN 1476-4660, URL <https://doi.org/10.1038/nmat1327>.
- ⁴⁷ I. Affleck, T. Kennedy, E. H. Lieb, and H. Tasaki, Communications in Mathematical Physics **115**, 477 (1988), ISSN 1432-0916, URL <https://doi.org/10.1007/BF01218021>.
- ⁴⁸ D. P. Arovas, Physics Letters A **137**, 431 (1989), ISSN 0375-9601, URL <http://www.sciencedirect.com/science/article/pii/0375960189909213>.
- ⁴⁹ I. Affleck, T. Kennedy, E. H. Lieb, and H. Tasaki, Phys. Rev. Lett. **59**, 799 (1987), URL <https://link.aps.org/doi/10.1103/PhysRevLett.59.799>.
- ⁵⁰ S. Moudgalya, S. Rachel, B. A. Bernevig, and N. Regnault, Phys. Rev. B **98**, 235155 (2018), URL <https://link.aps.org/doi/10.1103/PhysRevB.98.235155>.
- ⁵¹ J. D'Emidio, M. S. Block, and R. K. Kaul, Phys. Rev. B **92**, 054411 (2015), URL <https://link.aps.org/doi/10.1103/PhysRevB.92.054411>.
- ⁵² P. Kim, H. Katsura, N. Trivedi, and J. H. Han, Phys. Rev. B **94**, 195110 (2016), URL <https://link.aps.org/doi/10.1103/PhysRevB.94.195110>.
- ⁵³ D. C. Ronquillo, A. Vengal, and N. Trivedi, Phys. Rev. B **99**, 140413 (2019), URL <https://link.aps.org/doi/10.1103/PhysRevB.99.140413>.
- ⁵⁴ N. D. Patel and N. Trivedi, Proceedings of the National Academy of Sciences **116**, 12199 (2019), ISSN 0027-8424, <https://www.pnas.org/content/116/25/12199.full.pdf>, URL <https://www.pnas.org/content/116/25/12199>.
- ⁵⁵ M. Fishman, S. R. White, and E. M. Stoudenmire, *The itensor software library for tensor network calculations* (2020), 2007.14822.
- ⁵⁶ G. Alvarez, Computer Physics Communications **180**, 1572 (2009).

Supplemental: Gapless to gapless phase transitions by mode fractionalization in quantum spin chains

This supplemental contains the following sections. Section I detailed derivation of ULS's fermionic representation. Section II shows the derivation of the universal critical field h_{c2} at the boundary of B-phase and polarized phase. Section III analyzes the convergence of our results with both the number of DMRG kept states m and with respect to the thermodynamic limit. Section IV describes the contents of the data sources packaged in `sourcesPaper103.tar.xz` provided with this supplemental, and explains how to obtain, configure, compile, link, and run the DMRG++ computer program to reproduce the dynamical results. We have also added a description of the inputs provided in `inputsPaper103.tar.xz` that are helpful in obtaining the dynamical figures. *This supplemental and supporting files is also available at <https://g1257.github.io/papers/103>.*

I. FERMIONIZATION OF ULS MODEL

In this section we show a detailed derivation of ULS's fermionic representation. Rewriting the Hamiltonian in the fermion language allows us readily notice the SU(3) symmetry as mentioned in the main text, and is a useful tool in finding conserved charges that is not explicit otherwise. For spin-1 sites, define spin-1 operator $\mathbf{S}_i = \psi_i^\dagger \vec{S} \psi_i$, where \vec{S} is spin matrix in spin-1 Hilbert space:

$$S^z = \begin{pmatrix} 1 & 0 & 0 \\ 0 & 0 & 0 \\ 0 & 0 & -1 \end{pmatrix}, \quad S^+ = \begin{pmatrix} 0 & \sqrt{2} & 0 \\ 0 & 0 & \sqrt{2} \\ 0 & 0 & 0 \end{pmatrix} \quad (S1)$$

and $\psi = (d_{i,1}, d_{i,0}, d_{i,-1})^T$, with $d_{i,m}(d_{i,m}^\dagger)$ being fermion annihilation (creation) operator of spin- m at site i . So we have

$$S^z = d_1^\dagger d_1 - d_{-1}^\dagger d_{-1} \quad (S2)$$

$$S^+ = (S^-)^\dagger = \sqrt{2} (d_1^\dagger d_0 + d_0^\dagger d_{-1}) \quad (S3)$$

There is a constraint that the spin on each site is 1, thus

$$\frac{1}{2} \mathbf{S}^2 = \frac{1}{2} S^z S^z + \frac{1}{4} (S^+ S^- + S^- S^+) = (n - n_0 n_1 - n_0 n_{-1} - n_1 n_{-1}) \stackrel{!}{=} 1 \quad (S4)$$

where n_m is the *on-site* occupation number operator of m -type fermion, and $n_i = \sum_m b_{im}^\dagger b_{im}$ being the total *on-site* occupation number operator. The standard ULS Hamiltonian in spin language is written as

$$H_{ULS} = \sum_{\langle ij \rangle} \mathbf{S}_i \cdot \mathbf{S}_j + (\mathbf{S}_i \cdot \mathbf{S}_j)^2 - 2I \quad (S5)$$

note the identity I is spanned in $3 \otimes 3$ Hilbert space. The on-site identity is $I_0 = \sum_\alpha \langle \alpha | I_0 | \alpha \rangle d_\alpha^\dagger d_\alpha = \sum_\alpha d_\alpha^\dagger d_\alpha = n$, hence $I = n_i n_j$. Therefore we can make use of the fermion representation of identity as auxiliary parameters. Let us define a diagonal constant $c = n_i n_j + 3n_i$, then the equivalent ULS Hamiltonian \mathcal{H} can be expressed by.

$$\begin{aligned} \mathcal{H}_{ULS} &= H_{ULS} - c = \sum_{\langle ij \rangle} \mathbf{S}_i \cdot \mathbf{S}_j + (\mathbf{S}_i \cdot \mathbf{S}_j)^2 - c \\ &= \sum_{\langle ij \rangle} d_{i,1}^\dagger d_{i,1} d_{j,1}^\dagger d_{j,1} + d_{i,0}^\dagger d_{i,0} d_{j,1}^\dagger d_{j,0} + d_{i,-1}^\dagger d_{i,-1} d_{j,-1}^\dagger d_{j,-1} + d_{i,1}^\dagger d_{i,0} d_{j,0}^\dagger d_{j,1} + d_{i,0}^\dagger d_{i,-1} d_{j,-1}^\dagger d_{j,0} \\ &+ \sum_{\langle ij \rangle} d_{i,1}^\dagger d_{i,-1} d_{j,-1}^\dagger d_{j,1} + d_{i,0}^\dagger d_{i,1} d_{j,1}^\dagger d_{j,0} + d_{i,-1}^\dagger d_{i,0} d_{j,0}^\dagger d_{j,-1} + d_{i,-1}^\dagger d_{i,1} d_{j,1}^\dagger d_{j,-1} \\ &= - \left[\sum_{\langle ij \rangle} d_{i,1}^\dagger d_{j,1} d_{j,1}^\dagger d_{i,1} + d_{i,0}^\dagger d_{j,0} d_{j,1}^\dagger d_{i,0} + d_{i,-1}^\dagger d_{j,-1} d_{j,-1}^\dagger d_{i,-1} + d_{i,1}^\dagger d_{j,0} d_{j,0}^\dagger d_{i,1} + d_{i,0}^\dagger d_{j,-1} d_{j,-1}^\dagger d_{i,0} \right. \\ &+ \left. \sum_{\langle ij \rangle} d_{i,1}^\dagger d_{j,-1} d_{j,-1}^\dagger d_{i,1} + d_{i,0}^\dagger d_{j,1} d_{j,1}^\dagger d_{i,0} + d_{i,-1}^\dagger d_{j,0} d_{j,0}^\dagger d_{i,-1} + d_{i,-1}^\dagger d_{j,1} d_{j,1}^\dagger d_{i,-1} \right] \\ &= - \sum_{\langle ij \rangle; mm'} b_{i,m}^\dagger b_{j,m} b_{j,m'}^\dagger b_{i,m'} = - \sum_{\langle ij \rangle} (\psi_i^\dagger \psi_j) (\psi_j^\dagger \psi_i) \end{aligned} \quad (S6)$$

It is then obvious that \mathcal{H}_{ULS} remains invariant under transformations in $SU(3) \equiv \{U \in GL(3, \mathbb{C}) | U^\dagger U = \mathbb{I}, \det(U) = 1\}$.

Next we show the 3 conserved quantities explicitly by the fermion representation. To do this, we are going to calculate the commutation relation $[\mathcal{H}_{ULS}, \sum_i d_{in}^\dagger d_{in}] \equiv [\mathcal{H}_{ULS}, N_n]$. For simplicity, we choose only one neighboring pairs at site 1 and site 2 and the commutator of full system can be known by induction. Hence we only need to evaluate

$$\begin{aligned} [\mathcal{H}_{ULS}, N_n] &= \sum_{mm'} [d_{1m}^\dagger d_{1m'} d_{2m} d_{2m'}^\dagger, d_{1n}^\dagger d_{1n}] \\ &\quad + \sum_{mm'} [d_{1m}^\dagger d_{1m'} d_{2m} d_{2m'}^\dagger, d_{2n}^\dagger d_{2n}] \end{aligned} \quad (\text{S7})$$

where $N_n = d_{1n}^\dagger d_{1n} + d_{2n}^\dagger d_{2n}$ is the total occupation number of n -type fermion in the whole system (in the simplified case there are only 2 sites). It is straightforward to calculate:

$$[N_n, \mathcal{H}_{ULS}] = \left[\sum_n d_n^\dagger d_n, \mathcal{H}_{ULS} \right] = 0 \quad (\text{S8})$$

That is, the total occupation number N_m of $m = -1, 0, 1$ are good quantum numbers separately.

II. PROOF OF $h_{c2} = 4$

The critical value h_{c2} is the lowest field at which the BLBQ system becomes fully saturated. For this to happen, the sector with $S_z = L - 1$ has to have lower energy than the sector with $S_z = L$, and the field needed satisfies

$$E_{BLBQ}(L) - h_{c2}L = E_{BLBQ}(L - 1) - h_{c2}(L - 1), \quad (\text{S9})$$

where $E_{BLBQ}(L')$ is the ground state energy of BLBQ Hamiltonian without field in sector $S_z = L'$. We'll use PBC, which coincides with OBC in the thermodynamic limit $L \rightarrow \infty$. The sector with $S_z = L$ has only one state, with all spins having $m = 1$, and then the total energy contribution from H_{BLBQ} is $E_{BLBQ} = (1 - \beta)L$. Now sector with $S_z = L - 1$ has exactly L states, and all states have $L - 1$ spins with $m = 1$ and one spin with $m = 0$. We call $|k_p\rangle$ the state with $m = 0$ in the p -th site. Then

$$H_{BLBQ} |k_p\rangle = |k_{p+1}\rangle + |k_{p-1}\rangle + [(1 - \beta)L - 2] |k_p\rangle, \quad (\text{S10})$$

which can be solved by a Fourier transform. The $|S_z = L - 1\rangle$ ground state can then be written as

$$|S_z = L - 1\rangle = \frac{1}{\sqrt{L}} \sum_p (-1)^p |k_p\rangle, \quad (\text{S11})$$

with energy $(1 - \beta)L - 4$; using Eq. (S9) yields $h_{c2} = 4$.

Moreover, the Von Neumann entropy of the ground state of the $S_z = L - 1$ sector is exactly equal to $\ln(2)$, and that of the fully saturated state is 0. Therefore, the Von Neumann entropy has a discontinuity at $h = hc2 \equiv 4$, as expected, due to the first order nature of the transition.

III. SIZE EFFECTS AND CONVERGENCE

This section provides evidence that the results presented in the paper are converged. We analyze convergence first with the DMRG parameter m , the number of kept states. Figure S1 shows a comparison of the S^+S^- dynamics for the ULS model at zero field and with $L = 60$ sites for (a) $m = 500$ and (b) $m = 100$ states, indicating that none of the details discussed in the paper is affected by doubling the number of kept states, so that we have worked with correct accuracy for the level of detail needed to make the conclusions reached in the paper.

Figure S1 also shows the effect of increasing the number of sites from (a) $L = 60$ to (c) $L = 80$ to (d) $L = 100$ while maintaining a constant $m = 500$. Again, no relevant changes are noticeable that would change the conclusions reached in the paper.

Note that although $m = 500$ is enough for the convergence of dynamical structure factors, it turned out that, for the ULS critical point, we need significantly larger amount of kept states to produce an accurate von Neumann

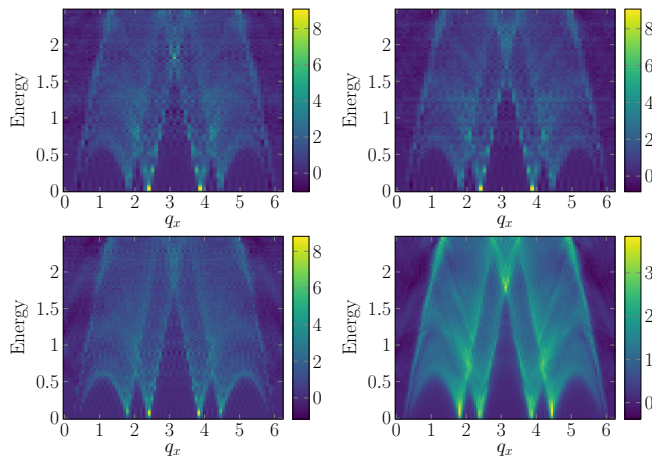


FIG. S1: S^+S^- dynamics for the ULS model at zero field for Above, left: $L = 60$ sites, $m = 500$ kept states; Above, right: $L = 60$ sites, $m = 1000$ kept states; Below, left: $L = 80$ sites, $m = 500$ kept states; Below, right: $L = 100$ sites, $m = 500$ kept states.

entanglement entropy $S(n)$ that is able to capture the correct central charge. In order to get the central charge for ULS model, we kept $m = 3000$ states which produces the expected $c = 2$ for the $SU(3)$ WZW theory. In contrast, smaller $m < 2000$ will give a fitted central charge $c < 2$ though it captures other dynamic/static features with good accuracy. This discrepancy of kept states between central charge calculation and other dynamical/static signature is highly likely to originate from the fine figures of oscillation term $S^{OSC}(n)$ under OBC, though the envelope from S^{CFT} only needs a much smaller m .

IV. DATA SOURCES

Data sources are distributed with supplemental. In file `inputsPaper103.tar.xz` we include input files to be delivered to DMRG++ for all figures in the main text and supplemental. In `sourcesPaper103.tar.xz` we include data and tex file for generating static and dynamical structure factors of ULS, AKLT and spin-1 Heisenberg model, and their SMA analysis and central charge.

The DMRG++ computer program⁵⁶ can be obtained with:

```
git clone https://github.com/g1257/dmrgpp.git
```

and PsimagLite with:

```
git clone https://github.com/g1257/PsimagLite.git
```

To compile:

```
cd PsimagLite/lib; perl configure.pl; make
cd ../../dmrgpp/src; perl configure.pl; make
```

The documentation can be found at <https://g1257.github.io/dmrgPlusPlus/manual.html> or can be obtained by doing `cd dmrgpp/doc; make manual.pdf`. The data needed for all the figures is in `RawData.tar.gz`. To reproduce figure 2, a ground state run needs to be made with `./dmrg -f akltGsL60Field0.ain` where all inputs are in `RawData.tar.gz`. After the ground state run has finished, the batches and inputs for all frequency runs can be generated with

```
export PSC=/path/to/dmrgpp/scripts
perl -I${PSC} ${PSC}/manyOmegas.pl InputDollarizedAkltL60Field0.inp batchDollarized.pbs test
```

that can be launched by replacing `test` with `submit`. When all frequency runs have finished, the post-processing to obtain the `.pgfplots` files is (after setting PSC as before)

```
perl -I${PSC} ${PSC}/procOmegas.pl -f InputDollarizedAkltL60Field0.inp -p
```

At zero field, we can add the symmetry sector `TargetSzPlusConst=` line, which should equal to $Sz + L$, where Sz is the symmetry sector to be targeted, and L the number of sites. We use Sz plus the constant L so that the number is always a non-negative integer. At non-zero field, the local symmetry Sz is also conserved, but we may not know what value it should take, and therefore we do not provide the line `TargetSzPlusConst=` in the input file, so that the diagonalization includes all symmetry sectors.
